Caged Compounds of Hydrolysis-Resistant Analogues of cAMP and cGMP: Synthesis and Application to Cyclic Nucleotide-Gated Channels

Volker Hagen,*,‡ Claudia Dzeja,§ Stephan Frings,§ Jürgen Bendig,|| Eberhard Krause,‡ and U. Benjamin Kaupp§

Forschungsinstitut für Molekulare Pharmakologie, Alfred-Kowalke-Strasse 4, D-10315 Berlin, Institut für Biologische Informationsverarbeitung, Forschungszentrum Jülich, Postfach 1913, D-52425 Jülich, and Institut für Organische und Bioorganische Chemie, Humboldt-Universität Berlin, D-10115 Berlin, Germany

Received December 8, 1995; Revised Manuscript Received March 18, 1996[⊗]

ABSTRACT: Photolabile compounds which rapidly release cAMP or cGMP after photolysis are widely used for *in situ* studies of signaling pathways inside cells. We synthesized two novel caged compounds, 4,5-dimethoxy-2-nitrobenzyl 8-Br-cAMP (caged 8-Br-cAMP) and 4,5-dimethoxy-2-nitrobenzyl 8-Br-cGMP (caged 8-Br-cGMP), which respectively release the hydrolysis-resistant analogues 8-Br-cAMP and 8-Br-cGMP. Their usefulness for physiological studies was examined in a mammalian cell line expressing the cyclic nucleotide-gated (CNG) ion channel of bovine olfactory sensory neurons. The synthesis procedure resulted in diastereomeric mixtures which were chromatographically separated into the axial and equatorial isomers of caged 8-Br-cAMP and of caged 8-Br-cGMP. The axial isomers which have a higher solubility and better solvolytic stability than the equatorial forms were used for experiments with CNG channels. Flashes of UV light produced steps in the concentration of 8-Br-cGMP which activated currents through CNG channels. Concentration steps inside the cell could be calibrated precisely using the relation between the ligand concentration and the normalized current. Similar results were obtained with caged 8-Br-cAMP. Control experiments with caged cGMP showed that flash-induced currents decayed within a few minutes because photoreleased cGMP was degraded by endogenous phosphodiesterase activity. The rise time of the 8-Br-cGMP-activated whole-cell current was consistent with a bimolecular reaction between channel and ligand.

Cyclic nucleotides, i.e., cAMP and cGMP, control a variety of important cellular processes [for reviews see Walter (1989) and Lincoln and Cornwell (1993)]. The principal targets of cyclic nucleotides are cAMP- and cGMP-dependent kinases (cAK and cGK; Walter, 1989; Taylor et al., 1990), cAMP- and cGMP-regulated phosphodiesterases (PDE; Beavo & Houslay, 1990), cyclic nucleotide-gated (CNG) ion channels (Yau & Baylor, 1989; Kaupp, 1995; Zimmerman, 1995), and transcription factors (Kolb et al., 1993). The study of cAMP- and cGMP-signaling pathways has been greatly facilitated by the design of chemical derivatives, such as phosphothioates (Eckstein, 1985) and "caged" compounds (Adams & Tsien, 1993; Corrie & Trentham, 1993). The popular term *caged* refers to molecules whose biological recognition or activity has been disabled by chemical modification. Photolysis cleaves the modifying group and rapidly releases the active molecule. Caged cyclic nucleotides have been first synthesized and physiologically tested by Korth and Engels (1979) and successfully employed in photolysis experiments to study a cAMP-dependent slow Ca^{2+} current in the heart (Nargeot et al., 1983; Nerbonne et al., 1984). Caged cAMP and caged cGMP have been also used to study the activation kinetics of the cGMP-gated channel from rod photoreceptor cells (Karpen et al., 1988), the signaling pathways in olfactory sensory neurons (OSNs) (Lowe & Gold, 1993), and the enhancement of Cl^- currents in ventricular cells (Ono et al., 1993).

In these studies, caged compounds have been used which release either cAMP or cGMP. Most cells are equipped with a powerful phosphodiesterase activity which rapidly degrades cyclic nucleotides and thus prevents a persistent cellular activation. Moreover, the low quantum efficiency of photolysis of many caged compounds limits the size of the concentration step that can be produced inside a cell by pulsed conventional light sources. For many physiological studies, caged compounds would be useful which liberate hydrolysis-resistant derivatives of higher biological efficacy than cAMP or cGMP. Suitable derivatives which meet these criteria are 8-Br-cAMP and 8-Br-cGMP. They are poorly hydrolyzable by phosphodiesterases, and 8-Br-cGMP activates cGK (Corbin et al., 1986) and CNG channels (Koch & Kaupp, 1985; Zimmerman et al., 1985; Tanaka et al., 1989) more effectively than cGMP.

Here we describe the synthesis and properties of 4,5-dimethoxy-2-nitrobenzyl derivatives (Figure 1) of 8-Br-cAMP (in the following referred to as caged 8-Br-cAMP) and of 8-Br-cGMP (caged 8-Br-cGMP) which respectively release 8-Br-cAMP and 8-Br-cGMP after irradiation with ultraviolet light. The usefulness of these compounds was tested in a mammalian cell line expressing the α-subunit of the CNG channel from bovine OSNs (Ludwig et al., 1990). Due to the high sensitivity of this channel for these ligands, light flashes of moderate intensity were sufficient to completely activate the channel. However, activation proceeded much more slowly than activation of rod and olfactory CNG channels in excised membrane patches (Karpen et al., 1988; Zufall et al., 1993). The slow rise time of the flash-induced current depends on 8-Br-cGMP concentrations and is the

‡ Forschungsinstitut für Molekulare Pharmakologie.
§ Forschungszentrum Jülich.
|| Humboldt-Universität Berlin.
⊗ Abstract published in *Advance ACS Abstracts,* May 15, 1996.

S0006-2960(95)02895-9 CCC: $12.00

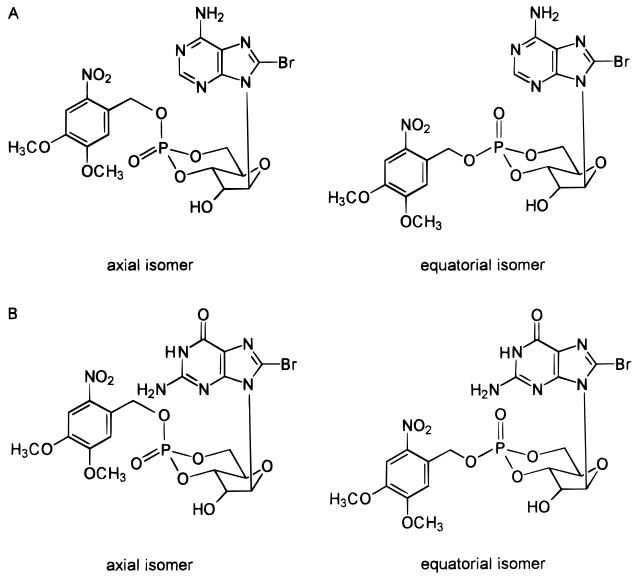

FIGURE 1: Structures of diastereoisomers of 4,5-dimethoxy-2-nitrobenzyl 8-Br-cAMP (A) and 4,5-dimethoxy-2-nitrobenzyl 8-Br-cGMP (B).

result of the low ligand concentrations available to activate the olfactory channel.

MATERIALS AND METHODS

Materials. Guanosine cyclic 3′,5′-monophosphate (cGMP, sodium salt) and 8-bromoadenosine cyclic 3′,5′-monophosphate (8-Br-cAMP) were purchased from Sigma (U.S.A.). 1-(2-Nitrophenyl)ethyl guanosine cyclic 3′,5′-monophosphate (caged cGMP) was purchased from Calbiochem (U.S.A.). 4,5-Dimethoxy-2-nitrobenzyl ATP was purchased from Molecular Probes (U.S.A.). 6-Nitroveratraldehyde was from Lancaster (England). Hydrazine monohydrate and MnO_2, activated for oxidations, were obtained from E. Merck (Germany). Dowex 50 WX-2 (100−200, H^+-form) was from Serva (Germany). Thin-layer chromatography (TLC) plates, Silica 60-F_{254}, were purchased from E. Merck (Germany). Silica gel for flash chromatography was from J. T. Baker (The Netherlands). All solvents from J. T. Baker (U.S.A.) were HPLC grade. All other chemicals were reagent grade. Water was purified with a Milli Q system (Millipore, Germany).

Synthesis of 8-Bromoguanosine Cyclic 3′,5′-Monophosphate (8-Br-cGMP). 1.836 g (5 mmol) of cGMP (sodium salt) was brominated with 1 g (6.25 mmol) of Br_2 by a procedure similar to the method of Mian et al. (1974). The sodium salt of 8-Br-cGMP (dihydrate, 1.93 g, 4 mmol, yield 80%) thus obtained was dissolved in deionized water and converted to the acid form by treatment with Dowex 50 WX-2 (H^+-form). Filtration, concentration, and lyophilization gave the pure free acid as white powder (1.66 g, 3.61 mmol, yield 90.25%). Anal. Calcd for $C_{10}H_{11}BrN_5O_7P\cdot 2H_2O$ (460.13): C, 26.10; H, 3.29; N, 15.22. Found: C, 26.05; H, 3.09; N, 15.31.

Synthesis of 4,5-Dimethoxy-2-nitrobenzyl 8-Bromoguanosine Cyclic 3′,5′-Monophosphate (Caged 8-Br-cGMP). A mixture of 8-Br-cGMP dihydrate (184 mg, 0.4 mmol) and approximately 3 mmol of 4,5-dimethoxy-2-nitrobenzyldiazomethane, freshly prepared from 900 mg (4 mmol) of 4,5-dimethoxy-2-nitrobenzylhydrazone (synthesized by treatment of 6-nitroveratraldehyde with hydrazine monohydrate in ethanol) and 5.8 g (60 mmol) of MnO_2 (90%) in 120 mL of chloroform by the procedure of Wootton and Trentham (1989) was stirred in 15 mL of DMSO at room temperature in the dark for 40 h. Monitoring of the reaction by TLC in a chloroform/methanol (5:1 v/v) solvent system revealed the appearance of a pair of spots with R_f 0.54 and 0.60, corresponding to the equatorial and the axial isomers of caged 8-Br-cGMP, respectively. DMSO, unreacted diazo compound, and reaction products with low polarity were removed by repetitive extraction with 60 mL of ether. The residual material which, among other substances, contained unreacted nucleotide and the axial and equatorial isomers in a 59:41 ratio, was dissolved in a minimal amount of chloroform and separated by flash chromatography on a silica column (3 × 30 cm). Elution using 100% chloroform and methanol/chloroform (95:5 v/v) removed hydrophobic side products of 4,5-dimethoxy-2-nitrobenzyldiazomethane from the column. Eluting with methanol/chloroform (90:10 v/v) gave fractions 1, 2, and 3 containing the axial isomer and mixtures of the axial and equatorial isomers, respectively. The fractions were dried on a rotary evaporator. Lyophilization gave 35 mg of the axial form (purity > 98.5%, <0.1% contamination by 8-Br-cGMP) and 12 mg of the equatorial form (purity > 92%, ∼6% contamination by the axial isomer, <0.2% contamination by 8-Br-cGMP) of caged 8-Br-cGMP as well as 78 mg of a mixture of the two isomers (purity >98%, <0.2% contamination by 8-Br-cGMP). The overall yield was 45%. The axial and the equatorial forms of caged 8-Br-cGMP were isolated directly with higher purity by preparative reversed-phase HPLC from the crude product or from the combined fractions 1, 2, and 3 after flash chromatography (Figure 2).

Axial 4,5-Dimethoxy-2-nitrobenzyl 8-Br-cGMP. ^{31}P NMR (DMSO-d_6) δ −5.17; ^{1}H NMR (DMSO-d_6) δ 3.86 (s, 3H, OCH_3), 3.89 (s, 3H, OCH_3), 4.21 (m, 1H, CH), 4.37 (m, 1H, CH), 4.69 (m, 1H, CH), 5.02 (m, 2H, CH_2), 5.53 (d, 2H, benzylic CH_2), 5.75 (s, 1H, CH), 6.33 (d, 1H, OH), 6.39 (br s, 2H, NH_2), 7.31 (s, 1H, aromatic CH), 7.73 (s, 1H, aromatic CH), 10.85 (br s, 1H, NH); UV (H_2O) λ_{max} 250 nm, 346 nm; mass spectrum 619.3 $[M + H]^+$. Anal. Calcd for $C_{19}H_{20}BrN_6O_{11}P_1\cdot 2H_2O$ (655.32): C, 34.82; H, 3.69; N, 12.82. Found: C, 34.85; H, 3.51; N, 12.44.

Equatorial 4,5-Dimethoxy-2-nitrobenzyl 8-Br-cGMP. ^{31}P NMR (DMSO-d_6) δ −4.27; ^{1}H NMR (DMSO-d_6) δ 3.90 (s, 3H, OCH_3), 3.96 (s, 3H, OCH_3), 4.42 (m, 3H, CH and CH_2), 4.72 (m, 1H, CH), 4.85 (t, 1H, CH), 5.34 (q, 1H, CH), 5.47 (d, 2H, benzylic CH_2), 5.70 (s, 1H, CH), 6.25 (d, 1H, OH), 6.75 (br s, 2H, NH_2), 7.30 (s, 1H, aromatic CH), 7.75 (s, 1H, aromatic CH), 10.67 (br s, 1H, NH); UV (H_2O) λ_{max} 250 nm, 346 nm; mass spectrum 619.3 $[M + H]^+$. Anal. Calcd for $C_{19}H_{20}BrN_6O_{11}P\cdot 2H_2O$ (655.32): C, 34.82; H, 3.69; N, 12.82. Found: C, 34.38; H, 3.41; N, 12.27.

Synthesis of 4,5-Dimethoxy-2-nitrobenzyl 8-Bromoadenosine Cyclic 3′,5′-Monophosphate (Caged 8-Br-cAMP). This compound was prepared following the same procedure described above for caged 8-Br-cGMP, from 8-Br-cAMP (163 mg, 0.4 mmol) and 3 mmol 4,5-dimethoxy-2-nitrobenzyldiazomethane. 21 mg of the axial isomer, 10 mg of the equatorial isomer, and 95 mg of a mixture of the two diastereoisomers were obtained using flash chromatography and lyophilization. The overall yield was 51%, and the isomers were formed in a 56 (axial):44 (equatorial) ratio. Preparative reversed-phase HPLC permitted complete sepa-

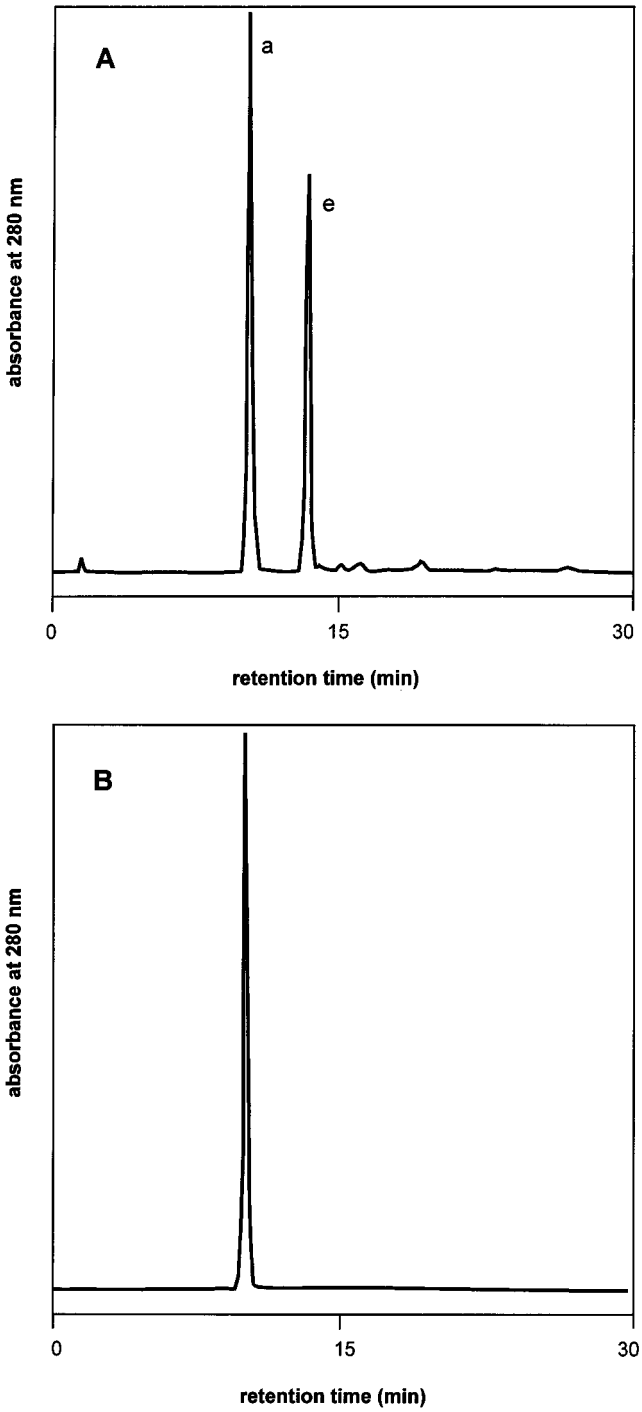

FIGURE 2: Reversed-phase HPLC profiles of 4,5-dimethoxy-2-nitrobenzyl 8-Br-cGMP. (A) Mixture of the axial (peak a, retention time 10.2 min) and the equatorial isomers (peak e, retention time 13.2 min) after flash chromatography (pooled fractions 1, 2, and 3). The retention time for 8-Br-cGMP was 1.4 min. (B) HPLC profile of the purified axial isomer after preparative HPLC and lyophilization; See Materials and Methods for details of the chromatographic procedure.

ration of the axial and the equatorial form. The final products were not contaminated by 8-Br-cAMP (<0.05%).

Axial 4,5-Dimethoxy-2-nitrobenzyl 8-Br-cAMP. TLC, R_f 0.71 (chloroform/methanol, 5:1 v/v); ^{31}P NMR (DMSO-d_6) δ −5.19; ^{1}H NMR (DMSO-d_6) δ 3.85 (s, 3H, OCH_3), 3.90 (s, 3H, OCH_3), 4.26 (m, 2H, CH_2), 4.66 (m, 1H, CH), 4.95 (t, 1H, CH), 5.41 (m, 1H, CH), 5.50 (d, 2H, benzylic CH_2), 5.86 (s, 1H, CH), 6.40 (d, 1H, OH), 7.32 (s, 1H, aromatic CH), 7.51 (br s, 2H, NH_2), 7.76 (s, 1H, aromatic CH), 7.85 (s, 1H, aromatic CH); UV (H_2O) λ_{max} 250 nm, 262 nm, 345 nm; mass spectrum 603.3 $[M + H]^+$. Anal. Calcd for $C_{19}H_{20}Br\,N_6O_{10}P{\cdot}H_2O$ (621.3): C, 36.73; H, 3.57; N, 13.53. Found: C, 36.37; H, 3.41; N, 13.12.

Equatorial 4,5-Dimethoxy-2-nitrobenzyl 8-Br-cAMP. TLC, R_f 0.61 (chloroform/methanol, 5:1 v/v); ^{31}P NMR (DMSO-d_6) δ −3.37; ^{1}H NMR (DMSO-d_6) δ 3.88 (s, 3H, OCH_3), 3.94 (s, 3H, OCH_3), 4.41 (m, 2H, CH_2), 4.71 (m, 1H, CH), 5.03 (t, 1H, CH), 5.44 (m, 1H, CH), 5.48 (d, 2H, benzylic CH_2), 5.88 (s, 1H, CH), 6.37 (d, 1H, OH), 7.26 (s, 1H, aromatic CH), 7.51 (br s, 2H, NH_2), 7.73 (s, 1H, aromatic CH), 8.19 (s, 1H, aromatic CH); λ_{max} 250 nm, 262 nm, 345 nm; mass spectrum 603.3 $[M + H]^+$. Anal. Calcd for $C_{19}H_{20}Br\,N_6O_{10}P{\cdot}H_2O$ (621.3): C, 36.73; H, 3.57; N, 13.53. Found: C, 36.48; H, 3.29, N, 12.97.

NMR spectra were performed at 200 MHz on a Varian Gemini 200 spectrometer. ^{1}H chemical shifts are given in ppm (δ) relative to tetramethylsilane as internal standard. Mass spectra were measured by electrospray ionization mass spectrometry in the positive ionization mode using a TSQ 700 (Finnigan MAT) spectrometer.

Reversed-Phase HPLC. Characterization of the diastereoisomers of caged 8-Br-cAMP and caged 8-Br-cGMP by analytical reversed-phase HPLC (RP-HPLC) was carried out with a PLRP-S column, 120 × 4.6 mm i.d., 8 μm (Polymer Laboratories Ltd., U.K.), with a Jasco gradient HPLC system (Jasco GmbH, Germany) consisting of two PU-980 pumps, a mixing chamber, an AS-950 autoinjector, and a UV-975 detector operating at 280 nm. The sample concentration was 1 mg/mL, and the injection volume was 20 μL. Runs were performed at ambient temperature and with a flow rate of 1 mL/min. The caged 8-Br-cAMP and caged 8-Br-cGMP isomers were eluted using a linear gradient of 20%−80% B in 40 min; eluent A, water; eluent B, acetonitrile.

Purification of 20 mg samples of the caged compounds was carried out by preparative HPLC on PLRP-S, 10 μm, 250 × 25 mm i.d. (Polymer Laboratories Ltd., U.K.) using a Shimadzu LC-8A system. Separations were performed at a flow rate of 10 mL/min using a linear gradient of 20%−60% B in 70 min; eluent A, water; eluent B, acetonitrile. The axial and equatorial isomers were isolated by lyophilization to give final products >99.9% purity (<0.05% contaminated by 8-Br-cAMP or 8-Br-cGMP) as determined by RP-HPLC analysis.

Half-Life Measurements in H_2O. Freshly prepared 25 μM solutions of the two forms of caged 8-Br-cAMP and the axial form of caged 8-Br-cGMP as well as a 10 μM solution of the equatorial isomer of caged 8-Br-cGMP in 5% acetonitrile/0.01 M HEPES/KOH buffer, pH 7.2, containing 0.12 M KCl were placed in the dark at 20 °C and monitored by HPLC at the start and at various time intervals up to several days. Additionally, solutions of the caged 8-Br-cGMP isomers in 5% acetonitrile/0.01 M sodium phosphate buffer, pH 4.6, and 5% acetonitrile/0.01 M sodium phosphate buffer, pH 7.2, were investigated. The results are shown in Table 1.

Stability. The diastereoisomers of caged 8-Br-cAMP and caged 8-Br-cGMP in their lyophilized form (hydrates or dihydrates) were stored at −24 °C and at room temperature for 3 months in the absence of light. Monitoring of the samples by HPLC showed that the axial isomers are more stable than the equatorial isomers (Table 2).

Solubility. The diasteroisomers of caged 8-Br-cAMP and caged 8-Br-cGMP were tested for their solubilities at room

Table 1: Calculated Half-Lives ($t_{1/2}$) of 4,5-Dimethoxy-2-nitrobenzyl Esters of 8-Br-cAMP and 8-Br-cGMP in Aqueous Buffer/Acetonitrile (95:5)

cyclic nucleotide ester	aqueous buffer	pH	$t_{1/2}$ (h)
4,5-dimethoxy-2-nitrobenzyl 8-Br-cAMP			
axial isomer	HEPES/KCl	7.2	60
equatorial isomer	HEPES/KCl	7.2	8
4,5-dimethoxy-2-nitrobenzyl 8-Br-cGMP			
axial isomer	HEPES/KCl	7.2	50
axial isomer	phosphate	7.2	50
axial isomer	phosphate	4.6	50
equatorial isomer	HEPES/KCl	7.2	5
equatorial isomer	phosphate	7.2	6
equatorial isomer	phosphate	4.6	5

Table 2: Degradation of 4,5-Dimethoxy-2-nitrobenzyl Esters of 8-Br-cAMP and 8-Br-cGMP Hydrates to 8-Br-cAMP and 8-Br-cGMP, Respectively, at −24 °C and at Room Temperature during Storage for 3 Months

cyclic nucleotide ester	temperature	degradation product (%)
4,5-dimethoxy-2-nitrobenzyl 8-Br-cAMP		8-Br-cAMP
axial isomer	−24 °C	<0.1
axial isomer	room temperature	0.7
equatorial isomer	−24 °C	<0.1
equatorial isomer	room temperature	6.2
4,5-dimethoxy-2-nitrobenzyl 8-Br-cGMP		8-Br-cGMP
axial isomer	−24 °C	<0.1
axial isomer	room temperature	7
equatorial isomer	−24 °C	4
equatorial isomer	room temperature	25

temperature using HPLC in 5% acetonitrile/0.01 M HEPES/KOH buffer, pH 7.2, containing 0.12 M KCl. After sonication to disperse solid material in the buffer and subsequent centrifugation, the concentrations of the axial and the equatorial isomers of the caged compounds were measured using HPLC.

Photolysis of the Diastereoisomers of Caged 8-Br-cGMP and Caged 8-Br-cAMP (Quantum Yield Determinations). The photolysis was carried out using a high-pressure mercury lamp (HBO 500, Oriel, U.S.A.) with controlled light intensity and a metal interference filter of 333 nm (Carl Zeiss, Germany). The irradiation spectra were recorded with a U-3410 spectrophotometer (Hitachi, Japan) combined with a computer and the software package SPECTRACALC. The irradiated solutions were analyzed using HPLC. 75 μM solutions of the two diastereoisomers of caged 8-Br-cAMP or the axial isomer of caged 8-Br-cGMP in 5% acetonitrile/0.01 M HEPES/KOH buffer, containing 0.12 M KCl, pH 7.2, and a 50 μM solution of the equatorial isomer of caged 8-Br-cGMP in 33% dioxane/0.01 M sodium phosphate buffer, pH 7.2, were placed in quartz cuvettes and irradiated for periods of time ranging between 150 and 1500 s in steps of 150 s. At the start and after each irradiation the absorption spectra (Figure 3) and the concentrations of the caged compounds and of the liberated 8-Br-cAMP or 8-Br-cGMP were measured using HPLC. With respect to the equatorial forms of the caged compounds, the measured concentrations of liberated 8-Br-cAMP or 8-Br-cGMP and of the remaining caged compounds were corrected with a factor to account for thermal hydrolysis of the 4,5-dimethoxy-2-nitrobenzyl esters. Quantum yields Φ, defined as the ratio of caged molecules converted or 8-Br-cAMP and 8-Br-cGMP molecules formed to the amount of photons absorbed, were

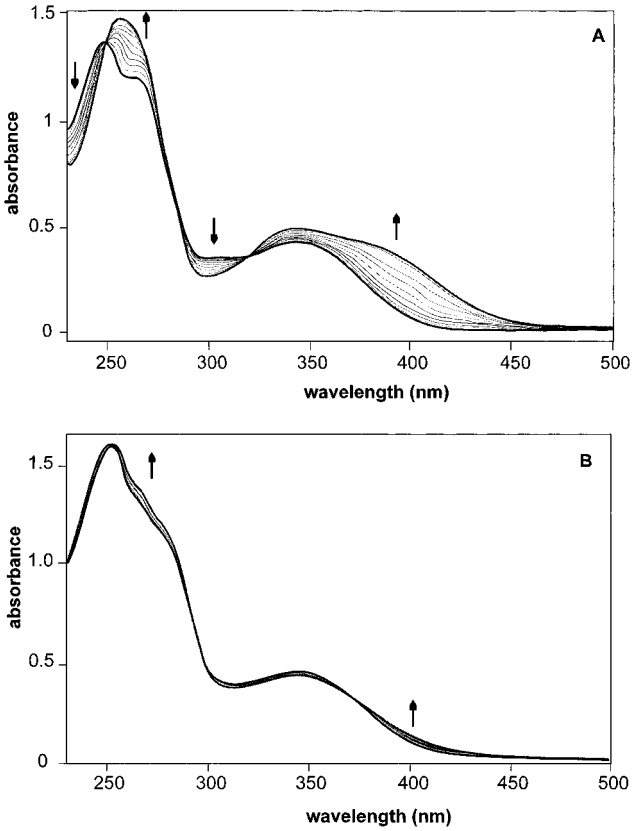

FIGURE 3: UV absorption spectra of the nonphotolyzed and photolyzed (150 s steps) axial isomers of 4,5-dimethoxy-2-nitrobenzyl 8-Br-cAMP (A) and 4,5-dimethoxy-2-nitrobenzyl 8-Br-cGMP (B). For experimental conditions see Materials and Methods. The arrows indicate the direction of the changes in absorbance with increasing irradiation times. The equatorial isomers of the two esters show absorption spectra that are almost identical to those of the corresponding axial isomers before and after photolysis.

determined by the relative method (Kuhn et al., 1989) according to the equation $\Phi_x = (dc/dt)_x \times (I_{abs})_x^{-1} \times V$ and using the standard *E*,*E*-1,4-diphenylbutadiene (1.3) ($\Phi_s = 0.11$; Schöneich et al., 1979). Subscripts s and x refer to standard and sample, respectively. The values of the reaction rate d*c*/d*t* (in mol L^{-1} s^{-1}) were calculated from the initial slope of the formation and/or decomposition curves (Figure 4). The value of I_{abs} (absorbed light intensity at $t = 0$ and $\lambda = 333$ nm in mol of "photons" s^{-1}), necessary for the calculation of the quantum yield Φ, was taken from the UV spectra (absorptivity in percent at $t = 0$ and $\lambda = 333$ multiplied by the photon flux I_o in mol s^{-1} at the irradiation position of the cuvette). I_o was determined by analyzing the irradiation spectra of the standard solution and using the equation $\Phi_s = (dc/dt)_s \times (I_{abs})_s^{-1} \times V$. For identical values of I_{abs} ($I_{abs,x} = I_{abs,s}$), the ratio of the calculated reaction rates is equal to the ratio of the quantum yields $\Phi_s/\Phi_x = (dc/dt)_s \times (dc/dt)_x^{-1}$. V is the volume of the irradiated solution (2 mL).

Electrophysiology. For flash photolysis experiments lyophilized caged 8-Br-cGMP (axial form) was dissolved in DMSO (1 mM) and was then diluted to a final concentration of 6.25 μM in the pipette solution containing 145 mM KCl, 8 mM NaCl, 1 mM $MgCl_2$, 2 mM MgATP, 0.3 mM GTP, 10 mM HEPES, and 0.02 mM EGTA, at pH 7.2 (KOH). The final DMSO concentration of ~0.7% had no effect on the whole-cell currents. Maintenance and transfection of human embryonic kidney (HEK 293) cells and recording of

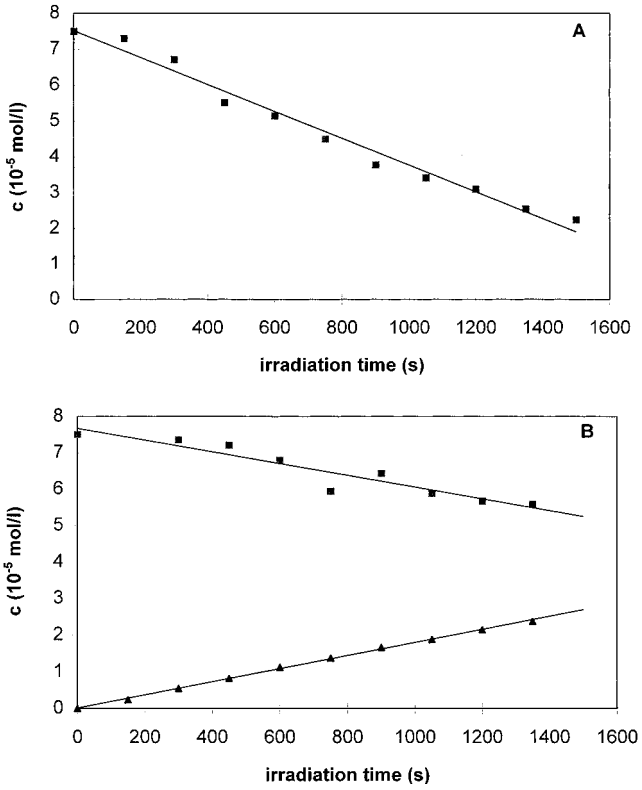

FIGURE 4: Photodecomposition of the axial isomers of 4,5-dimethoxy-2-nitrobenzyl 8-Br-cAMP (A, ■) and 4,5-dimethoxy-2-nitrobenzyl 8-Br-cGMP (B) as well as photorelease of 8-Br-cGMP from the caged 8-Br-cGMP compound (B, ▲) as function of irradiation time of the sample. Aqueous solutions of the esters were photolyzed and analyzed as described in Materials and Methods.

whole-cell current were as described (Frings et al., 1995). The cell interior was equilibrated for at least 5 min with the pipette solution containing the caged compound. The extracellular solution contained 120 mM NaCl, 3 mM KCl, 50 mM glucose, 10 mM HEPES, and 10 mM $MgCl_2$, at pH 7.4 (NaOH). Before irradiation of the cell with UV light, the extracellular perfusion medium was changed to a divalent free solution, containing 10 mM EGTA. In most experiments, caged compounds inside the cell were photolyzed with a 100 W mercury lamp (AMKO Germany, bulb HBO 103 W/2, Osram). The UV light was screened with a 335 nm cutoff filter (AMKO WG335). The duration of the light flash was controlled by a photoshutter (Compur, Germany). The UV light was fed into the epifluorescence port of a Nikon Diaphot microscope with a light guide. The light intensity above the magnifying objective (Nikon Fluor 40×, aperture, 1.3 mm) was 0.78 mW measured with a radiant power meter (Oriel; calibrated to light of $\lambda = 363$ nm, aperture 10 mm). In the experiment shown in Figure 10, the light intensity was 15−20 mW. A xenon flashlamp (AMKO) was employed for experiments designed to determine the time course of channel activation. The flash duration was about 1.5 ms. Light intensity was adjusted using quartz neutral density filters. Experiments with caged 8-Br-cAMP (axial form) and caged cGMP were similar, except that the concentrations in the pipette were higher (100 μM caged 8-Br-cAMP and 75 μM caged cGMP).

RESULTS

Chemical, Chromatographic, and Spectral Characteristics of Caged 8-Br-cAMP and Caged 8-Br-cGMP. 4,5-Dimethoxy-2-nitrobenzyl esters of 8-Br-cAMP and 8-Br-cGMP were prepared using a modification of the procedure described for the synthesis of the corresponding cAMP and cGMP esters (Nerbonne et al., 1984). The diastereomeric mixtures of the caged compounds (for structures see Figure 1) were chromatographically separated into the axial and equatorial isomers of the underlying dioxaphosphorinan ring. Isomeric species were assigned by ^{31}P NMR in analogy to the axial and equatorial isomers of cAMP and cGMP esters (Engels, 1979; Nerbonne et al., 1984). The ^{31}P NMR signals at higher field (−5.19 for caged 8-Br-cAMP and −5.17 for caged 8-Br-cGMP) correspond to the axial isomers, and those at lower field (−3.37 for caged 8-Br-cAMP and −4.27 for caged 8-Br-cGMP) correspond to the equatorial forms. The synthesis method led to a preferential formation of the axial isomers of the caged compounds, but all isomers were isolated in acceptable yields and high qualities (see Figure 2).

Irradiation of the axial and the equatorial forms of the 4,5-dimethoxy-2-nitrobenzyl esters of 8-Br-cAMP and 8-Br-cGMP at 300−350 nm in solution resulted in the liberation of free 8-Br-cAMP or 8-Br-cGMP anions, 4,5-dimethoxy-2-nitrosobenzaldehyde, and a proton. The photolysis mechanism is well-known (Kaplan et al., 1978; Engels, 1979; Corrie & Trentham, 1993). Differences between the diastereoisomers of caged 8-Br-cAMP and 8-Br-cGMP were observed with respect to the solubility in aqueous solutions. If the isomers were dissolved first in pure acetonitrile and then diluted into the appropriate HEPES buffer, saturation concentrations for the axial and the equatorial isomer of caged 8-Br-cAMP in 5% acetonitrile/0.01 M HEPES/KOH buffer, pH 7.2, were approximately 120 and 80 μM, respectively. The solvation procedure yielded saturation concentrations of approximately 100 and 10 μM, respectively, for the axial and the equatorial isomer of caged 8-Br-cGMP. The remarkably better solubilities of the axial isomers, in particular of caged 8-Br-cGMP, in aqueous solutions are an important advantage for their usage in cellular physiology studies. Moreover, the hydrates of the axial isomers were more stable than those of the equatorial isomers (see Table 2).

Hydrolysis of caged compounds was carried out in aqueous buffer solutions at 20 °C and was followed by HPLC. Neutral hydrolysis and hydrolysis at pH 4.6 to 8-Br-cAMP or 8-Br-cGMP proceeded with a time course consistent with a pseudo-first-order reaction. The calculated half-life times are shown in Table 1. The axial isomers are sufficiently stable with respect to the time needed for the photochemical or electrophysiological experiments. In contrast, the equatorial isomers of caged 8-Br-cAMP and caged 8-Br-cGMP hydrolyzed at pH 7.2 or 4.6 approximately 7−10 times faster than the respective axial isomers. These differences make the axial isomers of the 4,5-dimethoxy-2-nitrobenzyl esters of 8-Br-cAMP and 8-Br-cGMP more suitable for physiological experiments than the equatorial isomers or mixtures of the respective diastereoisomers. Solvolytic stability is an important feature of any good caged compound (Gurney & Lester, 1987) and particularly for 8-Br-cAMP and 8-Br-cGMP because these compounds are biologically very effective and because their degradation by endogenous phosphodiesterases proceeds at least 500 times more slowly than that of the natural cyclic nucleotides (Zimmerman et al., 1985).

Quantum Yield. The quantum efficiencies, Φ, of photolysis of the axial and the equatorial forms of caged 8-Br-cAMP and caged 8-Br-cGMP were determined by HPLC as described in Materials and Methods. Caged 8-Br-cAMP gave Φ values of 0.050 and 0.045, respectively, for the decay of the axial and the equatorial isomer. Φ values for the decay of the axial isomer of 4,5-dimethoxy-2-nitrobenzyl 8-Br-cGMP and the production of 8-Br-cGMP were 0.0049 and 0.0054, respectively. The Φ value for the decay of the equatorial isomer was 0.0052. Within the experimental accuracy, photolytic conversion of the two diastereoisomers of caged 8-Br-cAMP and the diastereoisomers of caged 8-Br-cGMP were identical. However, the efficiency of photorelease from the diastereoisomers of caged 8-Br-cAMP was 10-fold larger than from the diastereoisomers of the caged 8-Br-cGMP derivative. It is not yet known why 4,5-dimethoxy-2-nitrobenzyl 8-Br-cGMP is photolyzed to produce 8-Br-cGMP with only 10% of the efficiency of the corresponding 8-Br-cAMP ester, but the determined quantum yields correspond to those of 4,5-dimethoxy-2-nitrobenzyl cGMP and 4,5-dimethoxy-2-nitrobenzyl cAMP (Wootton & Trentham, 1989).

CNG Channel Activation by Photolysis of Caged 8-Br-cGMP. We tested caged 8-Br-cGMP in HEK 293 cells expressing the α-subunit of the CNG channel from bovine OSNs (Ludwig et al., 1990; Frings et al., 1995). 8-Br-cGMP is poorly hydrolyzed by endogenous PDE activity, and therefore concentrations of the caged compound in the pipette are limited by contamination with free 8-Br-cGMP, which activates CNG channels during equilibration of transfected HEK 293 cells with the pipette solution. By the time loading of cells was completed, freshly prepared solutions of caged 8-Br-cGMP were contaminated with ∼0.3%−0.7% 8-Br-cGMP. The optimal concentration of the caged compound is determined by this contamination and by the apparent affinity of the channel for 8-Br-cGMP. In order to determine $K_{1/2}$, we measured the relation between current and 8-Br-cGMP concentration using inside-out membrane patches of transfected HEK 293 cells that were sequentially exposed to solutions of increasing 8-Br-cGMP concentrations (Figure 5). The data were fitted to the Hill equation:

$$I/I_{max} = \frac{C^n}{C^n + K_{1/2}{}^n}$$

wherein I_{max} represents the current at saturating 8-Br-cGMP concentrations, C the concentration of 8-Br-cGMP, n the Hill coefficient, and $K_{1/2}$ the constant of half-maximal activation. Mean values ±sd (number of experiments) determined from Figure 5 were $K_{1/2} = 0.11 \pm 0.03$ μM and $n = 2.6 \pm 0.12$ (six experiments) at $V_m = +50$ mV, and $K_{1/2} = 0.13 \pm 0.03$ μM and $n = 2.6 \pm 0.12$ (nine experiments) at $V_m = -50$ mV. Thus, the olfactory CNG channel is roughly 12 times more sensitive for 8-Br-cGMP than for cGMP ($K_{1/2} = 1.36$ μM, $V_m = +80$ mV; Altenhofen et al., 1991). For the flash photolysis experiments, a concentration of 6.25 μM of caged 8-Br-cGMP was chosen, corresponding to a calculated content of uncaged 8-Br-cGMP of 18.75−43.75 nM. This contamination would activate less than 6% of the maximal current activated by 8-Br-cGMP.

Figure 6 shows a whole-cell recording of membrane current evoked by photolysis of caged 8-Br-cGMP. The cell

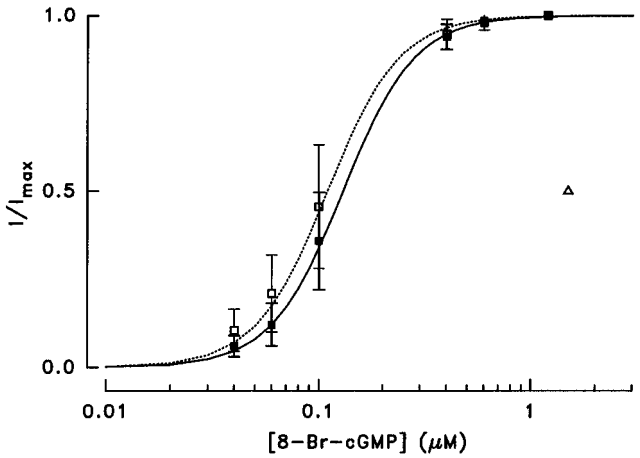

FIGURE 5: Dose−response relation of the heterologously expressed α-subunit of the olfactory CNG channel for 8-Br-cGMP. Steady-state 8-Br-cGMP-activated currents I measured from inside-out patches at +50 mV (□) and −50 mV (■) were normalized by the maximal current I_{max} at saturating 8-Br-cGMP concentrations. Data were obtained from six (+50 mV) and nine (−50 mV) experiments. Curves represent a least-squares fit of the Hill equation. Mean values ± sd of the constant of half-maximal activation $K_{1/2}$ and the Hill coefficient n were 0.11 ± 0.03 μM and 2.6 ± 0.1 for +50 mV and 0.13 ± 0.03 μM and 2.6 ± 0.1 for −50 mV. The open triangle indicates the $K_{1/2}$ value for cGMP at −80 mV [see Altenhofen et al. (1991)].

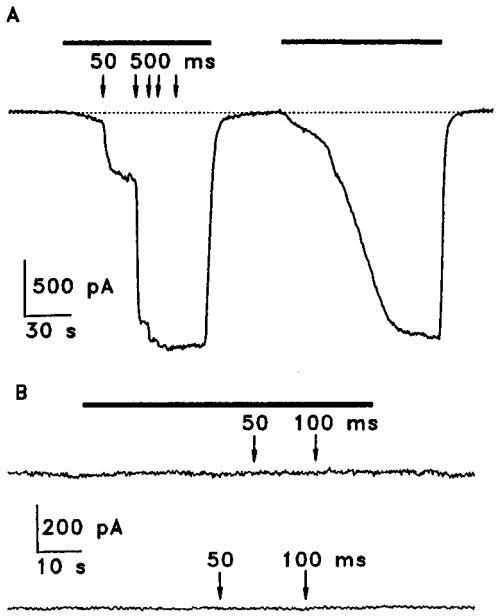

FIGURE 6: HEK 293 whole-cell current responses after photolysis of caged 8-Br-cGMP. (A) Current was activated by 50 and 500 ms flashes of UV-light (arrows). Black bars indicate superfusion of the cell with a Mg^{2+}-free solution. Recording pipette contained 6.25 μM caged 8-Br-cGMP. Membrane voltage was held at $V_m = -70$ mV. Initial Mg^{2+}-sensitive current was 106.5 pA, and the maximal current was 2154 pA. This corresponds to a 8-Br-cGMP contamination of 41 nM or 0.66%. (B) Control experiments with transfected HEK 293 cells and 100 μM caged ATP in the recording pipette (upper trace) and non-transfected HEK 293 cells with 6.25 μM caged 8-Br-cGMP in the recording pipette (lower trace); $V_m = -50$ mV.

was initially bathed in a solution containing 10 mM Mg^{2+} which effectively blocked currents activated by 8-Br-cGMP during equilibration of the cell with the caged compound (Frings et al., 1995). Shortly before illumination by UV light, the perfusion was switched to a solution that contained 10 mM EGTA. In most experiments, a small current of

several tens of picoampères developed after removal of Mg^{2+}. The small Mg^{2+}-sensitive currents are not due to the caged compound itself but are completely accounted for by the activation of CNG channels with contaminating 8-Br-cGMP. No or negligible Mg^{2+}-sensitive currents were observed in non-transfected cells or in cells which have been equilibrated with caged ATP (Figure 6B). This Mg^{2+}-sensitive current progressively increased during an experimental session due to solvolytic hydrolysis of caged 8-Br-cGMP. After 3 h at room temperature it can become as large as ~40% of the maximal photolysis-induced current corresponding to 2.2% (≅140 nM) 8-Br-cGMP (see dose−response curve in Figure 5). This result was confirmed by HPLC analysis of the pipette solutions (1.5%−2% 8-Br-cGMP content).

Upon irradiation of the cell with flashes of UV light (50 or 500 ms), large currents were recorded (Figure 6A). Several control experiments ascertained that these currents were activated by liberation of 8-Br-cGMP from the caged compound: (i) in the absence of the caged compound or in non-transfected HEK 293 cells, there was no current response to a light flash (Figure 6B); (ii) the light-evoked current responses were saturable. A 500-ms flash activated ≥90% of the maximal current; subsequent flashes caused much smaller increments of current or no changes at all. The current amplitude activated by a 50-ms flash was roughly 4 times smaller than that activated by a 500-ms flash (Figure 6A); (iii) the flash-induced current was almost entirely and reversibly suppressed by extracellular Mg^{2+} (Figure 6A); (iv) the nitrosobenzaldehyde photolysis product did not change the membrane conductance, because photolysis of caged ATP (100 μM), which has the same caging group as caged 8-Br-cGMP, was ineffective (Figure 6B). We conclude that the light-evoked current was activated by 8-Br-cGMP produced by the photolysis of caged 8-Br-cGMP.

The cyclic nucleotide-activated current was relatively constant for several minutes. Occasionally, the rapid increase in current was followed by a transient dip or a small decline to a lower plateau (see for sample Figures 8 and 9). We have not systematically examined the reason for this behavior. A similar yet larger current decline was observed by Karpen and co-workers (1988) in excised patches of photoreceptor membrane. These authors suggest that caged cGMP partitions into the membrane. After release of cGMP into the aqueous phase from the caged compound in the membrane, the cGMP concentration near the membrane should first increase and then decrease as diffusion into the cytosol proceeds.

Calibration of Flash-Induced Changes in 8-Br-cGMP Concentration. The photolysis-induced step in the 8-Br-cGMP concentration generated inside the cell can be accurately calibrated *in situ* by measuring the ratio $I_{h\nu}/I_{max}$ between the flash-induced current ($I_{h\nu}$) and the maximal current (I_{max}) at saturating 8-Br-cGMP concentrations. From the $I_{h\nu}/I_{max}$ ratio and the dose−response relation of Figure 5, the concentration step per flash was calculated. Figure 7 shows current recordings after repetitive irradiation with 50-ms flashes. The current amplitude incrementally increased with the number of flashes until it saturated after roughly ten flashes. A concentration jump of 38.4 ± 2.4 nM 8-Br-cGMP/flash was calculated from the first five flashes. The calibration of the flash-induced 8-Br-cGMP production *in situ* rests on the assumption that the ligand sensitivity is similar inside the cell and in excised membrane patches.

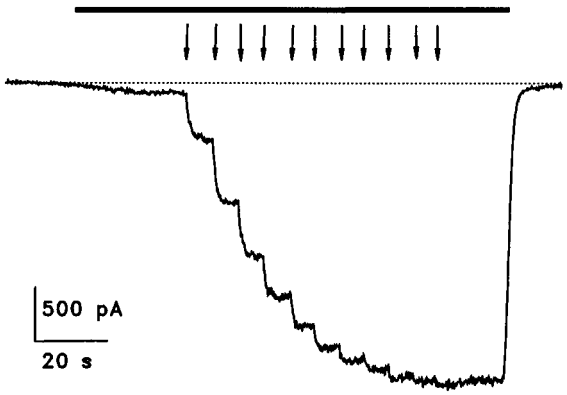

FIGURE 7: Calibration of current responses by successive flashes of UV light. Flash duration was 50 ms. Recording pipette contained 6.25 μM caged 8-Br-cGMP. The initial concentration of uncaged 8-Br-cGMP in the pipette solution was 34 nM, corresponding to a contamination of 0.54%. The concentration after the fifth flash was 226 nM. The average flash-induced increment of the 8-Br-cGMP concentration was 38.4 ± 2.4 nM (5); V_m = −50 mV.

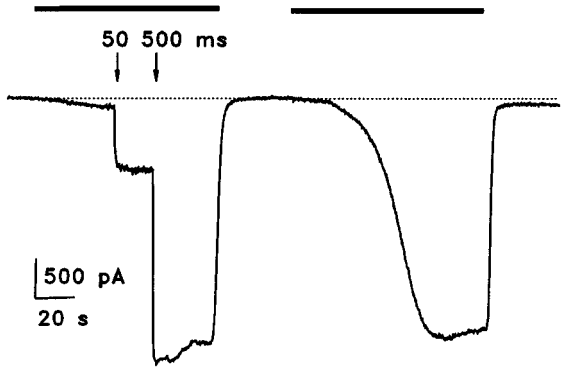

FIGURE 8: Flash-induced whole-cell current responses with caged 8-Br-cAMP. Recording pipette contained 100 μM caged 8-Br-cAMP. All other conditions as in Figure 6; V_m = −50 mV.

Ligand sensitivity of the olfactory CNG channel can be decreased by up to 20-fold by Ca^{2+}/calmodulin (Chen & Yau, 1994). The calmodulin effect is half-maximal at $[Ca^{2+}]_i$ of ~5 μM (Chen & Yau, 1994). The pipette and the bath solutions in the whole-cell configuration contained 0.02 mM and 10 mM EGTA, respectively. The $[Ca^{2+}]_i$ in HEK 293 cells under these conditions is ≤100 nM (Weyand et al., 1994), and changes in $[Ca^{2+}]_i$ are precluded.

CNG Channel Activation by Photolysis of Caged 8-Br-cAMP. Figure 8 shows an experiment with caged 8-Br-cAMP similar to that shown in Figure 6A with caged 8-Br-cGMP. A concentration of 100 μM caged 8-Br-cAMP was used because the channel is known to be ~30-fold less sensitive to 8-Br-cAMP than to 8-Br-cGMP. A 50-ms UV flash elicited a current of 800 pA. A second flash of 500-ms length evoked a larger current of roughly 3.5 nA. The flash-induced current was reversibly suppressed by 10 mM Mg^{2+} in the bath medium, and its amplitude decreased only slightly over a time period of several minutes (Figure 8).

CNG Channel Activation by Photolysis of Caged cGMP. Figure 9 shows a photolysis experiment with caged cGMP. Because the $K_1/_2$ constant of the olfactory channel for cGMP is ~12-fold larger than that for 8-Br-cGMP (see Figure 5), the pipette solution contained 75 μM caged cGMP. The flash-evoked currents differed from those with caged 8-Br-cGMP in that the rapid rise is followed by a slow decay.

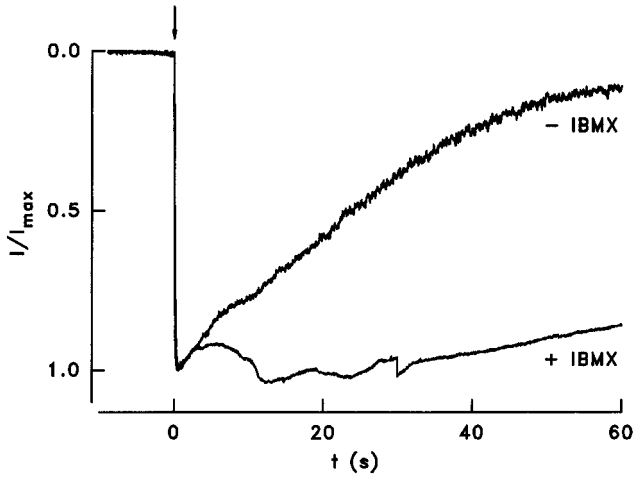

FIGURE 9: Flash-induced whole-cell current responses with caged cGMP in the presence and absence of the PDE inhibitor IBMX. Concentration of caged cGMP in the pipette was 75 μM; IBMX concentration in the pipette solution was 0.3 mM. Flash-induced currents measured from two different cells were normalized to the peak of the response shortly after the flash. Maximal whole-cell current in the absence of IBMX was 1.2 nA, and in the presence of IBMX it was 2.3 nA; $V_m = -50$ mV.

The time of half-maximal decay was $\tau_{1/2} = 34.1 \pm 15.6$ s (nine experiments), range 14.9−65.55 s. The current decline was almost completely abolished by 0.3 mM PDE inhibitor IBMX in the pipette solution. We interpret these results to indicate that cGMP released by light is hydrolyzed by endogenous PDE activity.

Time Course of Current Activation by 8-Br-cGMP. The kinetics of the channel response using caged 8-Br-cGMP are roughly 100-fold slower than in excised patches of salamander rod outer segments using caged cGMP (2−12 ms) (Karpen et al., 1988). We therefore analyzed the dependence of activation kinetics on 8-Br-cGMP concentration with flashes that were sufficiently short (20 ms) compared with the current rise time (≥200 ms). The light intensity was adjusted by neutral density filters. In a few experiments, one of which is shown in Figure 10A, photolysis was achieved with a xenon flashlamp (flash duration, ∼1.5 ms). No delay or S-shaped rise of the flash-induced current was observed at this time resolution (3 kHz; Figure 10A, inset), indicating that channel activation is not slowed by hindered diffusion as was reported for excised patches from rod outer segment membranes (Karpen et al., 1988). The current rise was fitted by two exponentials with time constants of $\tau_f =$ 44 ms and $\tau_s = 507$ ms and normalized amplitudes of $A_f =$ 0.15 and $A_s = 0.85$, respectively (see Figure 10A, legend). In most experiments, the fraction of the faster component was ≤0.2. A distinct fast component on the rising phase is also apparent in experiments with OSNs and caged cAMP (Lowe & Gold, 1993). The initial rising phase is probably caused by higher local concentrations of the lipophilic caged 8-Br-cGMP in the membrane than in the bulk.

The activation kinetics can be qualitatively understood by the following simple scheme [sequential binding of several cGMP molecules is ignored; for a more elaborate model see Karpen et al. (1988)]:

$$R + L \underset{k_d}{\overset{k_b[L]}{\rightleftharpoons}} (RL)_c \underset{k_c}{\overset{k_o}{\rightleftharpoons}} (RL)_o$$

The rate constant of channel opening, k_o, is of the order of

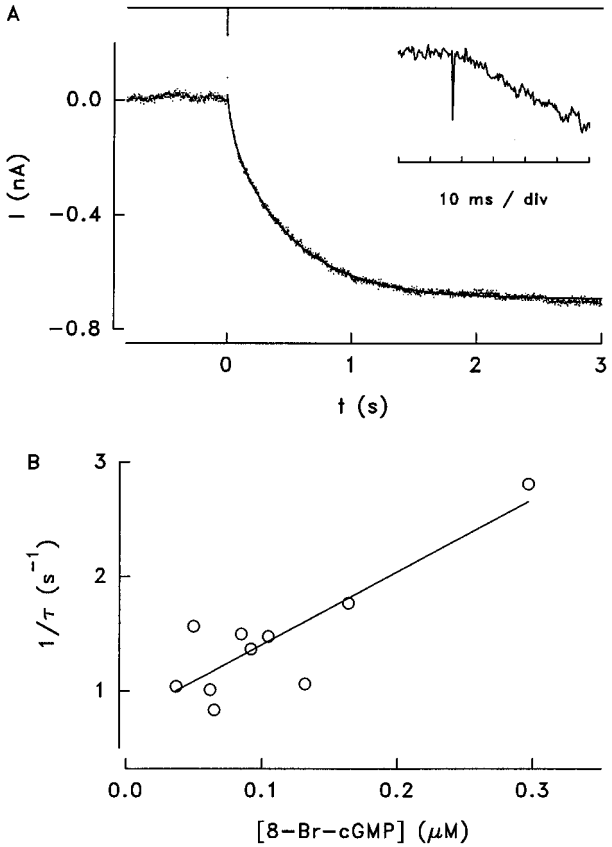

FIGURE 10: Time course of the current activated by photolysis of caged 8-Br-cGMP. (A) Current was activated by a 1.5 ms flash from a xenon flashlamp. The thin line represents a fit of the noisy current trace with two exponential time constants $\tau_f = 44$ ms and $\tau_s = 507$ ms. Normalized amplitudes were 0.15 and 0.85, respectively ($I_t/I_{max} = 1 - [A_f e^{-t/\tau_f} + A_s e^{-t/\tau_s}]$). Inset: same recording on an expanded time scale. (B) Concentration dependence of the reciprocal rise-time constant τ_s. Current was activated by 20 ms flashes of different light intensity; $V_m = -70$ mV.

10^4 s^{-1} (Karpen et al., 1988) and therefore cannot be rate-limiting for a process that takes several 100 ms. Assuming that the ligand-binding step is rate-limiting, the reciprocal of the rise time, $1/\tau$, is $k_b[L] + k_d k_c/(k_o + k_c)$. If $(k_o + k_c) \gg k_d k_c$, then the rate of current activation will solely be determined by the product $k_b[L]$ of the bimolecular rate constant of binding k_b and the ligand concentration [L]. As predicted by this simple relation, $1/\tau$ linearly increased with final 8-Br-cGMP concentration (Figure 10B). The slope yielded a value for k_b of about 6.4×10^6 M^{-1} s^{-1}, which reasonably agrees with a value of $\sim 5 \times 10^7$ M^{-1} s^{-1} for the reaction between the rod CNG channel and cGMP (Karpen et al., 1988). In conclusion, the slow activation is due to low 8-Br-cGMP concentrations and is compatible with fast channel activation in excised patches by much higher concentrations of cGMP.

DISCUSSION

We have described the preparation of caged derivatives of 8-Br-cAMP and 8-Br-cGMP and examined their usefulness for the study of cellular processes *in situ*. The principal advantage of 8-bromo-substituted derivatives of cyclic nucleotides is their hydrolysis-resistant nature. Caged derivatives of these compounds therefore allow persistent elevation of cyclic nucleotides *in situ*. The decay of the flash-induced concentration step is probably determined by slow dialysis

of the cell with the pipette solution and diffusion of liberated 8-Br-cGMP across the cell membrane rather than by PDE hydrolysis. The much higher efficacy of channel activation by 8-bromo-substituted derivatives, in principle, would be also beneficial, since the rather low quantum yield of this class of caged compounds limits the concentration step that can be produced by short flashes. However, for most purposes the contamination by "free" 8-Br-cAMP or 8-Br-cGMP, but also the lower solubility, sets a practical upper limit for the concentration of the caged compounds.

In this respect, caged cGMP is more convenient to use than caged 8-Br-cGMP. Residual free cGMP becomes degraded by endogenous PDE activity while the cell is equilibrated with the caged compound, or it can be removed beforehand by treatment of solutions with trypsin-activated PDE (Karpen et al., 1988). In addition, due to hydrolysis of the flash-generated cGMP, the experiment can be repeated many times as long as the cell contains sufficient caged cGMP. The hydrolysis-resistant nature of 8-Br-cGMP along with its high biological efficacy precludes such precautions and instead requires reagents of extremely high purity.

The rate of odor-induced cAMP accumulation in isolated olfactory cilia is very fast ($\leq$50 ms) (Breer et al., 1990; Jaworsky et al., 1995), whereas the time course of whole-cell currents in intact olfactory sensory neurons is slow and displays a delay of several hundred milliseconds (Firestein & Werblin, 1989; Firestein et al., 1990). These seemingly conflicting observations have led to the hypothesis that inherently slow channel kinetics determine the sluggish olfactory response (Zufall et al., 1993). In fact, using a rapid perfusion technique, these authors measured a current rise time of 2.5 ms in excised membrane patches that were exposed to brief pulses of 10 mM cGMP. Extrapolation of this rate to physiological changes in the cyclic-nucleotide concentration ($\leq$10 μM) yields rise times of the order of 2.5 s, whereas rates determined with caged 8-Br-cGMP predict time constants of $\sim$10 ms ($k = 10^7$ M^{-1} s^{-1} $\times$ 10^{-5} M $\cong$ 100 s^{-1}). Current changes measured by Zufall et al. (1993) exhibited a pronounced S-shaped time course, which may be indicative of solution mixing as the rate-limiting step under their experimental conditions. However, a k_b value of 7×10^6 M^{-1} s^{-1} for the reaction between the olfactory CNG channel and 8-Br-cGMP is nearly of the same order as a k_b value of 5×10^7 M^{-1} s^{-1} reported for activation of the CNG channel from rod photoreceptors by cGMP (Karpen et al., 1988). This comparison also suggests that no fundamental differences exist in this respect between activation of olfactory and rod CNG channels [see, however, Zufall et al. (1993)]. Our results do not support the proposal that channel kinetics are the sole determinant of the odor-induced response kinetics (Zufall et al., 1993). Instead, we conclude that odor-stimulated synthesis of cAMP in intact olfactory neurons proceeds at a much slower rate than has been measured in preparations of isolated olfactory cilia (Breer et al., 1990).

Caged derivatives of hydrolysis-resistant cyclic nucleotides expand the repertoire of techniques for the study of signaling by intracellular messengers. They can be used to discover novel cellular processes or targets that are modulated by cyclic nucleotides. In particular, they allow the study of modulation of CNG channels and protein kinase activity in their cellular context. For example, Ca^{2+} and cGMP concentrations in vertebrate photoreceptor cells are coupled by a complex network of enzymatic reactions [for review see Kaupp and Koch 1992)]. CNG channels are permeable to Ca^{2+}, and their closing by light is followed by a decrease in $[Ca^{2+}]_i$ which in turn stimulates the synthesis of new cGMP by a guanylate cyclase. Similarly, cAMP-hydrolyzing and cAMP-synthesizing pathways in OSNs are also modulated by $[Ca^{2+}]_i$ [for review see Shepherd (1994)]. With these novel caged compounds, it may be feasible to experimentally isolate modulation of CNG channel activity by Ca^{2+}/calmodulin (Hsu & Molday, 1993; Chen & Yau, 1994; Körschen et al., 1995), by phosphorylation/dephosphorylation reactions (Gordon et al., 1992, 1995) or by other cellular mechanisms independent of their modulation by the ligand itself. Finally, hydrolysis-resistant caged compounds of cAMP or cGMP will also facilitate studies of Ca^{2+} permeation in CNG channels which rely on fast activation of the channels (Frings et al., 1995).

ACKNOWLEDGMENT

We thank Drs. K.-W. Koch and R. Seifert (Jülich) for critical reading of the manuscript and helpful discussions.

REFERENCES

Adams, S. R., & Tsien, R. Y. (1993) *Annu. Rev. Physiol. 55*, 755−784.
Altenhofen, W., Ludwig, J., Eismann, E., Kraus, W., Bönigk, W., & Kaupp, U. B. (1991) *Proc. Natl. Acad. Sci. U.S.A. 88*, 9868−9872.
Beavo, J. A., & Houslay, M. D. (1990) in *Cyclic Nucleotide Phosphodiesterases: Structures, Regulation and Drug Action*, John Wiley & Sons, Ltd., Chichester, England.
Breer, H., Boekhoff, I., & Tareilus, E. (1990) *Nature 345*, 65−68.
Chen, T.-Y., & Yau, K.-W. (1994) *Nature 368*, 545−548.
Corbin, J. D., Ogreid, D., Miller, J. P., Suva, R. H., Jastorff, B., & Døskeland, S. O. (1986) *J. Biol. Chem. 261*, 1208−1214.
Corrie, J. E. T., & Trentham, D. R. (1993) in *Bioorganic Photochemistry, Vol. 2: Biological Applications of Photochemical Switches* (Morrison, H., Ed.) pp 243−305, John Wiley & Sons, Ltd., Chichester, England.
Eckstein, F. (1985) *Annu. Rev. Biochem. 54*, 367−402.
Engels, J. (1979) *Bioorg. Chem. 8*, 9−16.
Firestein, S., & Werblin, F. (1989) *Science 244*, 79−82.
Firestein, S., Shepherd, G. M., & Werblin, F. S. (1990) *J. Physiol. 430*, 135−158.
Frings, S., Seifert, R., Godde, M., & Kaupp, U. B. (1995) *Neuron 15*, 169−179.
Gordon, S. E., Brautigan, D. L., & Zimmerman, A. L. (1992) *Neuron 9*, 739−748.
Gordon, S. E., Downing-Park, J., Tam, B., & Zimmerman, A. L. (1995) *Biophys. J. 69*, 409−417.
Gurney, A. M., & Lester, H. A. (1987) *Physiol. Rev. 67*, 583−617.
Hsu, Y.-T., & Molday, R. S. (1993) *Nature 361*, 76−79.
Jaworsky, D. E., Matsuzaki, O., Borisy, F. F., & Ronnett, G. V. (1995) *J. Neurosci. 15*, 310−318.
Kaplan, J. H., Forbush, B., III, & Hoffman, J. F. (1978) *Biochemistry 17*, 1929−1935.
Karpen, J. W., Zimmerman, A. L., Stryer, L., & Baylor, D. A. (1988) *Proc. Natl. Acad. Sci. U.S.A. 85*, 1287−1291.
Kaupp, U. B. (1995) *Curr. Opin. Neurobiol. 5*, 434−442.
Kaupp, U. B., & Koch, K.-W. (1992) *Annu. Rev. Physiol. 54*, 153−175.
Koch, K.-W., & Kaupp, U. B. (1985) *J. Biol. Chem. 260*, 6788−6800.
Kolb, A., Busby, S., Buc, H., Garges, S., & Adhya, S. (1993) *Annu. Rev. Biochem. 62*, 749−795.
Körschen, H. G., Illing, M., Seifert, R., Sesti, F., Williams, A., Gotzes, S., Colville, C., Müller, F., Dosé, A., Godde, M., Molday, L., Kaupp, U. B., & Molday, R. S. (1995) *Neuron 15*, 627−636.

Korth, M., & Engels, J. (1979) *Naunyn−Schmiedeberg's Arch. Pharmacol. 310*, 103−111.

Kuhn, H. J., Braslavsky, S. E., & Schmidt, R. (1989) *Pure Appl. Chem. 61*, 187−210.

Lincoln, T. M., & Cornwell, T. L. (1993) *FASEB J. 7*, 328−338.

Lowe, G., & Gold, G. H. (1993) *J. Physiol. 462*, 175−196.

Ludwig, J., Margalit, T., Eismann, E., Lancet, D., & Kaupp, U. B. (1990) *FEBS Lett. 270*, 24−29.

Mian, A. M., Harris, R., Sidwell, R. W., Robins, R. K., & Khwaja, T. A. (1974) *J. Med. Chem. 17*, 259−263.

Nargeot, J., Nerbonne, J. M., Engles, J., & Lester, H. A. (1983) *Proc. Natl. Acad. U.S.A. 80*, 2395−2399.

Nerbonne, J. M., Richard, S., Nargeot, J., & Lester, H. A. (1984) *Nature 310*, 74−76.

Ono, K., Nakashima, Y., & Shioya, T. (1993) *Pfl*ügers *Arch. 424*, 546−548.

Schöneich, R., Bendig, J., & Kreysig, D. (1979) *Z. Naturforsch. 34A*, 1344−1351.

Shepherd, G. M. (1994) *Neuron 13*, 771−790.

Tanaka, J. C., Eccleston, J. F., & Furman, R. E. (1989) *Biochemistry 28*, 2776−2784.

Taylor, S. S., Buechler, J. A., & Yonemoto, W. (1990) *Annu. Rev. Biochem. 59*, 971−1005.

Walter, U. (1989) *Rev. Physiol. Biochem. Pharmacol. 113*, 41−88.

Weyand, I., Godde, M., Frings, S., Weiner, J., Müller, F., Altenhofen, W., Hatt, H., & Kaupp, U. B. (1994) *Nature 368*, 859−863.

Wootton, J. F., & Trentham, D. R. (1989) in *Photochemical Probes in Biochemistry* (Nielsen, P. E., Ed.) NATO ASI Ser. C, Vol. 272, pp 277−296, Kluwer Academic, The Netherlands.

Yau, K.-W., & Baylor, D. A. (1989) *Annu. Rev. Neurosci. 12*, 289−327.

Zimmerman, A. L. (1995) *Curr. Opin. Neurobiol. 5*, 296−303.

Zimmerman, A. L., Yamanaka, G., Eckstein, F., Baylor, D. A., & Stryer, L. (1985) *Proc. Natl. Acad. Sci. U.S.A. 82*, 8813−8817.

Zufall, F., Hatt, H., & Firestein, S. (1993) *Proc. Natl. Acad. Sci. U.S.A. 90*, 9335−9339.

BI952895B